Journal of Engineering Mathematics **28**: 21–42, 1994.

Turbulent spots in channel flows

D.S. HENNINGSON[1], A.V. JOHANSSON and P.H. ALFREDSSON
Department of Mechanics, Royal Institute of Technology, S-100 44 Stockholm, Sweden

Received 4 January 1993; accepted in revised form 15 August 1993

Abstract. A number of investigations into the formation and development of turbulent spots in plane Poiseuille, plane Couette and watertable flows are reviewed. Three main observations are drawn from this work. Firstly, the initial development is associated with the transient growth due to the three-dimensional lift-up effect. Secondly, the spreading and propagation velocities of the different spots are quite similar. Thirdly, the velocity field inside the spots show essentially all the characteristics of fully developed turbulent flow, albeit at low Reynolds numbers. The mechanism behind the rapid spreading of the spots, however, is not yet fully understood, although observations of wave activity, modifications of the surrounding flow field and stability calculations point in the direction of growth by destabilization.

1. Introduction

Transition to turbulence in wall-bounded shear flows follows essentially two different routes. The first, which we may call the secondary instability scenario, starts out with exponentially growing two-dimensional waves which subsequently become three-dimensional as a result of the secondary instability of the finite amplitude two-dimensional waves. The three-dimensional disturbances rapidly evolve into an array of Λ-vortices which in turn break down to turbulence. The classical experiments of Klebanoff et al. [1] clearly illustrates this scenario and the review article by Herbert [2] gives a theoretical background.

The second route to turbulence, which we along with Morkovin [3] call the bypass transition scenario, is not as well understood. This scenario is typically associated with large amplitude localized disturbances which quickly develop streaky structures, shear layers and strong vortices. The two-dimensional waves and their secondary instability is bypassed in this case. Growth of localized disturbances and their subsequent breakdown to turbulent spots are prominent features in natural transition to turbulence. Flow perturbations are then likely to be emanating from free-stream turbulence and/or spatially localized effects such as surface irregularities. The study of transition from localized disturbances has gained increased attention in recent years.

The first observations of turbulent spots were made by Emmons [4] in a water table flow, i.e. a flow of a thin water layer over an inclined plate. Turbulent spots have been studied extensively in the boundary layer geometry, see for example the review article by Riley and Gad-el-Hak [5]. For channel flows, however, the information has not until recently been as substantial. The present review concerns the formation and characteristics of spots in channel flows, i.e. in plane Poiseuille flow, water table flow and plane Couette flow. In all cases the situation is one of subcritical transition. In fact, plane Couette flow is linearly stable for all Reynolds numbers. Turbulent spots in plane Poiseuille flow were first studied by Carlson et al. [6], whereas the first studies of spots in plane Couette flow are the numerical and physical experiments of Lundbladh and Johansson [7] and Tillmark and Alfredsson [8],

respectively. In this review attention is also paid to the early formation stages and their underlying mechanisms.

2. Spot formation

2.1. Experimental findings

The experimental findings regarding the initial development of localized disturbances and incipient spots have to a large extent been carried out in the boundary layer geometry. As a motivation for the following theoretical discussion as well as for the work on channel flow disturbances, we start with a short description of some of the boundary layer results.

Amini and Lespinard [9] studied an incipient spot and found that streaks developed close to the wall. The streaks moved much faster than the wavepacket studied by Gaster and Grant [10]. Similar results were found by Chambers and Thomas [11] who also studied the breakdown of localized disturbances. They found that the disturbance consisted of both a wavepacket and a faster moving streaky part and that the turbulent breakdown was associated with the streaks rather than the wavepacket. They concluded that the wavepacket played a passive role in the transition process.

The breakdown process of the streaks was studied by Acarlar and Smith [12] who generated a disturbance by fluid injection. They found that the injected fluid caused streamwise streaks which subsequently formed strong vortices. In their investigation the interaction between the heads of the vortices and the stretched out legs of nearby vortices caused the final breakdown to turbulence. Similar strong vortices are found to develop during the secondary instability process, where they are also found to play an important role during late transitional and early turbulent flow (see e.g. Sandham and Kleiser [13]).

Breuer and Haritonidis [14] studied the evolution of weak disturbances created by a localized motion of the wall. They found both a dispersive wavepacket and a faster moving streaky transient part. The transient part was also associated with a sharp shear layer in the centre of the disturbance. In their experiments the transients were not strong enough to cause transition but died away leaving a slowly growing wave packet.

By limiting the amplitude of the initial disturbance it is also possible for the breakdown of a localized disturbance to be associated with the growth of the wavepacket. Cohen et al. [15] showed that when the waves in the wavepacket have grown to large enough amplitude they experience a Craik type resonance, a non-linear spread of energy into higher wavenumber components and a subsequent breakdown into a turbulent spot.

Thus wavepackets and streaks have both been observed in the initial development of localized disturbances. We will now consider the initial value problem for disturbances in parallel shear flows in order to illustrate the theoretical basis for these findings.

2.2. The initial value problem for localized disturbances

The equations for a localized disturbance on a base flow U_i satisfying the incompressible Navier–Stokes equations, can in tensor form be written,

$$\frac{\partial u_i}{\partial t} + U_j \frac{\partial u_i}{\partial x_j} + u_j \frac{\partial U_i}{\partial x_j} + \frac{\partial p}{\partial x_i} - \frac{1}{\mathrm{Re}} \nabla^2 u_i = \frac{\partial}{\partial x_j}(u_i u_j)\,, \tag{1a}$$

$$\frac{\partial u_i}{\partial x_i} = 0\,, \tag{1b}$$

where $(u_1, u_2, u_3) = (u, v, w)$ are the disturbance velocities in the streamwise $(x_1 = x)$, normal $(x_2 = y)$ and spanwise $(x_3 = z)$ directions and p is the pressure. All quantities are made non-dimensional with a reference velocity (U_m) and the characteristic length (h), making $\mathrm{Re} = U_m h/\nu$. For plane Poiseuille flow U_m is the centreline velocity, for water table flow it is the free surface velocity and for Couette flow it is half of the velocity difference between the walls. The reference length h is taken as the channel half-height for Poiseuille and Couette flow and as the total depth of the fluid in the water table case.

In order to determine the growth mechanisms possible for the disturbance it is of interest to consider the equation for the total energy of the perturbation. It can be derived by multiplying (1a) with u_i and integrating over a volume containing the complete disturbance. The resulting so called Reynolds–Orr equation can be written

$$\frac{\mathrm{d}E_T}{\mathrm{d}t} = -\int_V u_i u_j \frac{\partial U_i}{\partial x_j}\,\mathrm{d}V - \frac{1}{\mathrm{Re}}\int_V \frac{\partial u_i}{\partial x_j}\frac{\partial u_i}{\partial x_j}\,\mathrm{d}V\,, \tag{2}$$

where $E_T = \frac{1}{2}\int_V u_i u_i\,\mathrm{d}V$. Note that the nonlinear terms on the right hand side of equation (1a), along with a number of the linear terms, have dropped out, which is the case as long as the disturbance vanish on the boundaries or for periodic boundary conditions[2]. The Reynolds–Orr equation shows that the relative change of the total energy is independent of the amplitude, i.e. at every instant the quantity $(1/E_T)(\mathrm{d}E_T/\mathrm{d}t)$ is unaffected by a rescaling of the amplitude. Hence, if *all* infinitesimal disturbances exhibit monotonical decay of the total energy this will also be the case for *all* finite amplitude disturbances. Conversely, if *any* finite amplitude disturbance exhibit total energy growth there must exist *an* instantaneously growing infinitesimal disturbance. We may formulate this important conclusion as follows:

> The total energy of a localized disturbance of arbitrary amplitude cannot grow without the existence of a linear growth mechanism.

The Reynolds number below which no growth is possible $(\mathrm{d}E/\mathrm{d}t < 0)$ will be denoted Re_g and the Reynolds number above which the linearized problem supports exponentially growing solutions will be called Re_c. The Reynolds number for which turbulent spots can first appear will be denoted Re_t.

Table 1 shows the values of these critical Reynolds numbers for the flows of interest here. It is evident that transition is usually subcritical, i.e. occurs for Reynolds numbers below

Table 1. Critical Reynolds numbers for some parallel shear flows. From top to bottom the values for Re_g are found by Joseph and Carmi [16] and Joseph [17], the values of Re_t by Alavyoon et al. [18], Lundbladh and Johansson [7], Tillmark and Alfredsson [8] and Gustavsson and Ögren [19] and the values of Re_c by Orszag [20], Herron [21] and Chin [22].

Flow	Re_g	Re_t	Re_c
Poiseuille	49.6	1100	5772
Couette	20.7	360	∞
Water table	–	1100	$\approx$5700*

* Depends slightly on a surface tension related parameter.

Re_c, and is thus dependent on some other *linear* growth mechanism than exponentially growing normal modes.

We turn to the linearized version of (1a) written in a form suitable for the parallel channel flow problems in order to describe such a linear mechanism. In parallel shear flows $U_i = U(y)\delta_{1i}$. If the equations are horizontally Fourier transformed they can be reduced into one equation governing the normal velocity ($\hat{v}$) and one for the normal vorticity ($\hat{\eta} = \mathrm{i}\beta\hat{u} - \mathrm{i}\alpha\hat{w}$), where α and β are the streamwise and spanwise wavenumber components and the caret signifies a Fourier transformed quantity. Introducing the vector $\mathbf{q} = (\hat{v}, \hat{\eta})^T$ the governing equations can be written

$$\mathcal{M}\frac{\partial \mathbf{q}}{\partial t} = \mathcal{L}\mathbf{q}\,, \qquad \mathcal{M} = \begin{pmatrix} -D^2 + k^2 & 0 \\ 0 & 1 \end{pmatrix}, \qquad \mathcal{L} = \begin{pmatrix} \mathcal{L}_{OS} & 0 \\ \mathrm{i}\beta U' & \mathcal{L}_{SQ} \end{pmatrix}, \tag{3}$$

where

$$\mathcal{L}_{OS} = -\mathrm{i}\alpha U(D^2 - k^2) + \mathrm{i}\alpha U'' + (D^2 - k^2)^2/\mathrm{Re}\,, \tag{4a}$$

$$\mathcal{L}_{SQ} = \mathrm{i}\alpha U - (D^2 - k^2)/\mathrm{Re}\,. \tag{4b}$$

Here $'$ and D denotes a derivative with respect to y and $k^2 = \alpha^2 + \beta^2$. The solution to (3) can be written formally as

$$\mathbf{q} = \sum_{n=1}^{\infty} \kappa_n \tilde{\mathbf{q}}_n \, \mathrm{e}^{-\mathrm{i}\omega_n t}\,, \tag{5}$$

where $\tilde{\mathbf{q}}_n$ and ω_n are the eigenfunctions and eigenvectors of $\mathrm{i}\mathcal{M}^{-1}\mathcal{L}$, respectively. They consist of both Orr–Sommerfeld and Squire modes. κ_n are the coefficients in the eigenfunction expansion of the initial condition $\hat{\mathbf{q}}_0$.

The energy density of the disturbance for a specific Fourier component can be written as (see Gustavsson [23])

$$E(t) = \frac{1}{k^2}\int_{y_1}^{y_2} (k^2|\hat{v}|^2 + |\hat{v}'|^2 + |\hat{\eta}|^2)\,\mathrm{d}y\,, \tag{6}$$

where the total energy E_T is recovered if the above expression is integrated over α and β. The maximum growth possible for any given time G(t) can be expressed

$$G(t) = \max_{E(0)\neq 0} \frac{E(t)}{E(0)}\,. \tag{7}$$

The growth function $G(t)$ can most easily be calculated if one projects the solution on the space spanned by the first N eigenfunctions of $\mathrm{i}\mathcal{M}^{-1}\mathcal{L}$. The procedure is described in Reddy and Henningson [24].

The typical behaviour of $G(t)$ for flows allowing subcritical instability can be seen in Fig. 1, where the growth function has been calculated for a supercritical (Re = 8000) and a subcritical (Re = 5000) Reynolds number in the Poiseuille flow case. For Re = 8000 the effect of the least stable eigenmode on the maximum growth envelope can be seen in the exponential behaviour for large times. Before that, however, large transient growth can be seen. For the subcritical case only the transient part of the growth remains whereas the

asymptotic exponential growth has turned to decay. It is clear that the transient growth depends on cancellation of nearly linearly dependent eigenmodes since each mode in the eigenfunction expansion (5) decays for Re = 5000. If all the initial energy is introduced only into the growing mode (Re = 8000) the lower curve is obtained. Thus even when linearly unstable modes exist it is of interest to examine the transient behaviour when the likelihood of transition is assessed.

The qualitative behaviour seen in Fig. 1 is also present for other parameter values, although the transient growth may be much larger than seen here. As we will see below, it is disturbances with no streamwise dependence ($\alpha = 0$) which grow most rapidly (see also Butler and Farrell [25]). From the argument above about the necessity of a linear growth mechanism for subcritical growth of arbitrary amplitude perturbations, it is clear that the transient growth will persist down to $\mathrm{Re} = \mathrm{Re}_g$. Thus it is this possibility for growth in the total disturbance energy which has to be exploited if subcritical transition is to occur.

The two possible growth mechanisms (modal and transient) give two types of behaviour for typical localized disturbances. The former results in the wavepacket type behaviour calculated by Gaster [26, 27]. This assumes that the transient phase has decayed and that only the least stable mode is important in the development, i.e. $\hat{v} = \kappa_1 \tilde{v}_1 \, \mathrm{e}^{-\mathrm{i}\omega_1 t}$. The solution in physical space can then be written

$$v = \frac{1}{4\pi^2} \int_\alpha \int_\beta \hat{v}(y; \alpha, \beta) \, \mathrm{e}^{\mathrm{i}\theta} \, \mathrm{d}\alpha \, \mathrm{d}\beta \qquad \theta = \left(\alpha \frac{x}{t} + \beta \frac{z}{t} - \omega_1 \right) t \,. \tag{8}$$

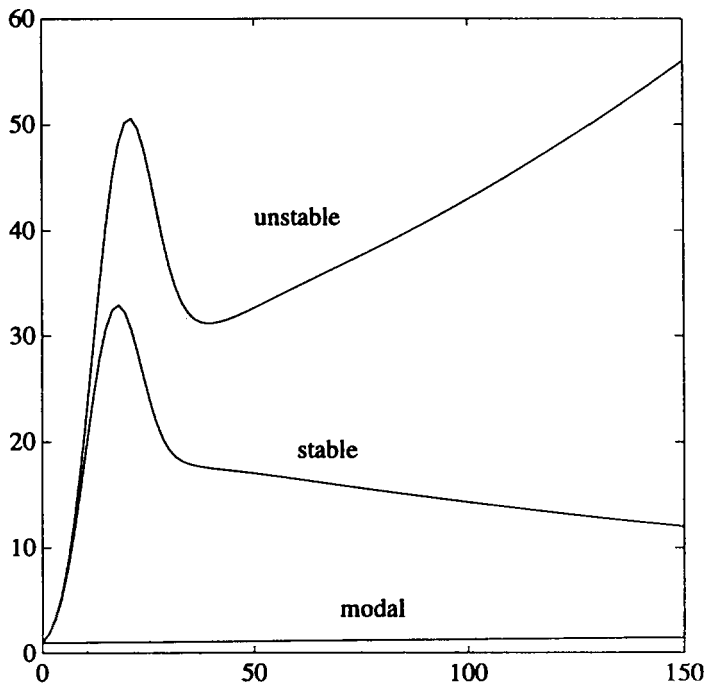

Fig. 1. Plot of $G(t)$ for stable and unstable Poiseuille flow. The stable case corresponds to $\alpha = 1$, $\beta = 0$, Re = 5000 and the unstable case to $\alpha = 1$, $\beta = 0$, Re = 8000. The curve labeled *modal* is a plot of the energy growth in the case that the initial velocity is the eigenfunction corresponding to the unstable eigenvalue for $\alpha = 1$, $\beta = 0$, Re = 8000. From Reddy and Henningson [24].

The inversion integrals can be calculated using the method of steepest descent and the solution shows the typical dispersive behaviour associated with a wavepacket. For the wavepacket the normal vorticity behaves in the same manner as the normal velocity.

In the transient part the main contribution to the growth comes from the normal vorticity (see e.g. Gustavsson [28]). The physical mechanism is vortex tilting of mean spanwise vorticity into normal vorticity by the normal velocity. This localized liftup is represented by the off-diagonal term in the matrix operator $\mathscr{L}$. It can be shown that this effect is largest for wavenumber components with $\alpha = 0$. Henningson et al. [29] shows that one may obtain the following result

$$\hat{\eta} = \sum_{n=1}^{N} \kappa_n \tilde{\eta}_n \, \mathrm{e}^{-\mathrm{i}\omega_n t} = \cdots = (\hat{\eta}_0 - \mathrm{i}\beta U' \hat{v}_0 t)[1 + O(t/R)] \,. \tag{9}$$

We have here assumed that $\alpha = 0$. This shows that the transient growth is connected to the algebraic instability discussed by Ellingsen and Palm [30] and Landahl [31]. They showed that inviscid disturbances grow algebraically without limit when wavenumbers along the β-axis are excited. This behaviour results in disturbances which are continuously stretched in the streamwise direction causing sharp shear layers which are damped on a viscous time scale.

2.3. Transient effects in channel flows

The transient effects described above are particularly important in channel flow transition since it is usually subcritical, see Table 1. We will here describe results from some recent investigations.

Henningson [32] studied the inviscid evolution of an infinitesimal localized disturbance in a piecewise linear approximation of Poiseuille flow. He found that the disturbance could be divided into one dispersive part, comprising the spreading of waves and one convective part, characterized by an advection of the disturbance with the local mean velocity. In a particular initial disturbance the advected part was found to be associated with a shear layer which did not decay but remained as a 'permanent scar' as predicted by Landahl [33]. These results are the same as those predicted for the boundary layer case (Gustavsson [34]).

Henningson et al. [35] and Henningson et al. [29] calculated the viscous development of localized disturbances and found that the transient growth increased dramatically with increasing amount of energy in low streamwise wavenumbers, as predicted by the theory presented above. The details of the dependence of finite amplitude growth on the linear mechanism was studied, and two main cases could be distinguished. Firstly, if the initial disturbance contained energy along the spanwise wavenumber axis, the amplitude of those wavenumbers grew rapidly due to the linear mechanism. Higher spanwise modes were also rapidly excited. Secondly, if the initial energy density along the spanwise wavenumber axis was low or vanishing, rapid growth of those Fourier components still occurred as soon as non-linear interactions had transferred energy to that area in wavenumber space. Thus the detailed dependence on the initial condition became largely eliminated. Henningson et al. [29] also made high resolution calculations valid all the way to the turbulent spot stage. It was found that the streaks containing normal vorticity were converted to strong vortices

tilted toward the streamwise direction. The spot stage was initiated by strong spikes in the normal velocity appearing on the streamwise vortices.

A typical disturbance development is seen in Fig. 2, taken from Henningson et al. [29]. The first four frames shows the early non-linear development prior to breakdown, whereas in the last frame a small turbulent spot has appeared. Figure 2a shows both the wavepacket and the much stronger streaks. It is indeed the streaks which break down to form the spot, while the wavepacket quickly is damped out in this linearly stable flow.

Klingmann [36] studied the development of localized disturbances experimentally in an air channel. She found three stages of development. A first rapid nonlinear redistribution stage where the smallest scales in the initially strong disturbance was damped out. A second stage which was essentially described by linear theory where streaky structures developed and a third breakdown stage where spikes formed and the disturbance became turbulent. The development found in the experiment and the high resolution calculations made in Henningson et al. [29] show close agreement. Klingmann also measured the spanwise wavenumber associated with the streaks. She found fairly broad peaks. This is well in accordance with the theoretical results which show that a broad range of spanwise wavenumbers experience rapid transient growth. The particular spanwise wavenumber peaks seen in an experiment or simulation depends significantly on the initial condition.

3. Growth of turbulent spots in channel flows

The overall characteristics of turbulent spots are their shape, propagation speeds and spreading rate. These characteristics depend on the basic flow but also on the Reynolds number, how far from the origin of spot formation the spot is observed and to some extent the initial disturbance. The spot affects the surrounding laminar flow in two ways. Firstly, it acts as a local blockage due to the higher wall shear inside the spot, thereby displacing the surrounding flow. Secondly, it radiates disturbances into the laminar flow.

In all channel flows (see Table 1) the transitional Reynolds number, Re_t, is smaller than the critical Reynolds number for growth of infinitesimal two-dimensional disturbances, Re_c. Natural formation of spots in these flows occurs due to background disturbances in the mean flow or surface roughness. In experiments a controlled disturbance, in the form of an injected pulse of fluid or in the case of water table flow a small drop of fluid hitting the free water surface, is usually used. This gives a space and time reference to the origin of the spot. Although the initial disturbances may be of different strength and size it is commonly believed that the asymptotic behaviour of the spot is independent of the initial disturbance, although its virtual origin may not coincide with the point of the disturbance. The streamwise propagation velocity of the front of the spot is usually higher than for the rear laminar-turbulent interface, so that the spot length increases as it travels downstream.

One important feature of turbulent spots is the rapid spanwise spreading into the surrounding laminar flow, much larger than what could be accounted for by turbulent diffusion. Typical half spreading angles are of the order of 10°, whereas turbulent diffusion normal to the wall in a turbulent boundary layer is around 1°. There is some evidence that the spot itself destabilizes the laminar flow surrounding it, and Gad-el-Hak, Blackwelder and Riley [37] named this 'growth by destabilization'. Several attempts to elucidate the

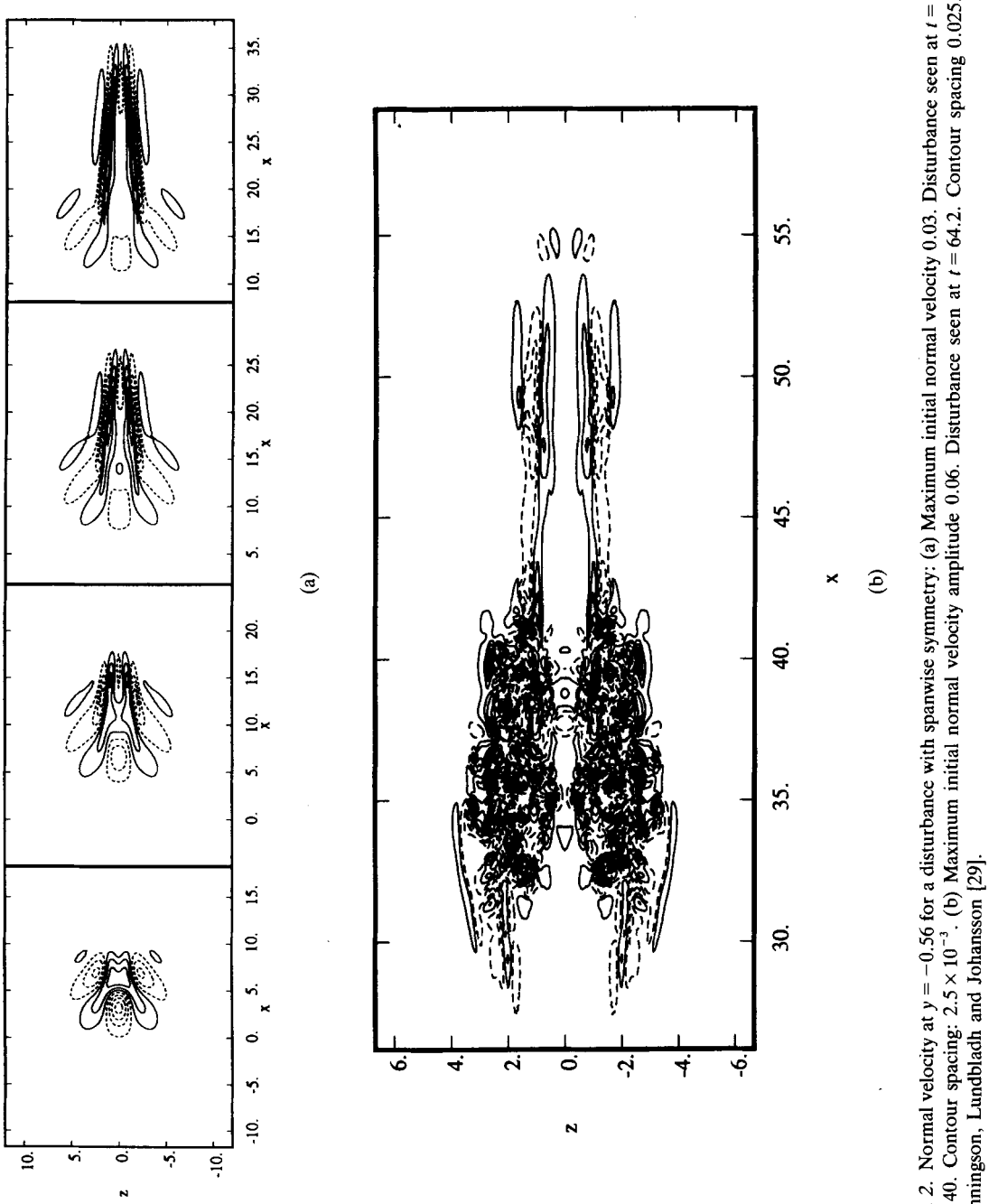

Fig. 2. Normal velocity at $y = -0.56$ for a disturbance with spanwise symmetry: (a) Maximum initial normal velocity 0.03. Disturbance seen at $t = 10$, 20, 30, 40. Contour spacing: 2.5×10^{-3}. (b) Maximum initial normal velocity amplitude 0.06. Disturbance seen at $t = 64.2$. Contour spacing 0.025. From Henningson, Lundbladh and Johansson [29].

mechanism behind the spreading has been advanced, some of which will be discussed below together with descriptions of the spot characteristics.

3.1. Water table flows

The first observation of turbulent spots were made by Emmons [4] in a water table flow. His observations established a qualitative picture of laminar-turbulent transition in channel flows, through disturbances that give rise to localized breakdown and formation of spots. In Emmons' experiment the spots were observed through the irregular surface waves created by the turbulence within the spot. Aside from the general shape of the spot, Emmons also noted that its propagation velocity was smaller than the maximum velocity of the flow and that its spanwise size increased linearly with downstream distance. Mitchner [38] continued Emmons work and reported a spreading rate of 6.6° for Re = 1230, and propagation speeds, 0.54 and 0.61 for the rear and forward parts of the turbulent region. Mitchner pointed out that the rear part of the spot was well defined whereas the downstream edge was more vague and that the shape of the spot was an isosceles triangle with its vertex pointing upstream. Mitchner also made measurements of artificially triggered spots in a laminar boundary layer and noted that they have an arrowhead shape pointing in the downstream direction in contrast to the water table spot.

Bertshy and Abernathy [39] presented photographs of water-table spots. They also showed that drag reducing polymers inhibit the spot growth. Gustavsson and Ögren [19] presented both photographs and measurement data of overall characteristics. The photographs were taken with a novel technique in which a photographic paper was placed below the water table glass surface (the room was dark) and a flash light was activated a certain time after the spot was triggered by a falling droplet. The photographs reflect the perturbations of the free surface, and showed a boomerang-like shape of the turbulent region. They presented data for three Re (1110, 1360 and 1910) that showed that the spreading angle increased with Re (becoming 7.6° at the highest Re) and that the propagation velocities were about 0.58 and 0.63, respectively. Gustavsson and Ögren also showed that at low Reynolds numbers the spot may grow asymmetrically, i.e. growth on one side may be larger than on the other.

Lindberg et al. [40] also used a water table but made the flow visualization with reflective flakes suspended in the water in order to obtain a more complete picture of the spot development. Some flow structures that were unnoticed in the previous studies were now revealed. For instance, the newly formed spot had an appearance very similar to that observed by Mitchner in a boundary layer flow. As the spot travelled downstream, however, the turbulence in the front part dies away, leaving at first a streamwise-oriented streaky pattern of small spanwise wave length, in front of the turbulent region. Lindberg et al. also showed that the spreading angle increases with Reynolds number for low Re. Above Re = 1500 the spreading angle was constant and in the range 8–9°, depending slightly on the inclination angle of the water table. They also carried out hot-film measurement which showed that the streamwise velocity profile in the laminar flow outside the wing-tip region is modified, and OS-calculations showed that the flow to some extent was destabilized.

3.2. Plane Poiseuille flow

In most plane Poiseuille flow experiments, transition to turbulence is usually found at Reynolds numbers between 1000 and 3000. The first flow visualization experiments that

revealed turbulent spots were made by Carlson et al. [6]. They used reflective flakes and presented detailed flow visualization photographs of spots at Reynolds numbers just above the transitional. These spots have an appearance slightly different from that of water-table spots, but are similar in the respect that the small scale turbulence is located in the rear part. However in front of this region, as well as outside the wingtips of the spot they observed wave packets of inclined waves with a wave length of the order of a few channel heights. The oblique waves at the wing-tips of the spots were observed to break down and this was assumed to be coupled to the spanwise spreading of the spot. Further downstream the photographs show that the central part of the spot seems to relaminarize, whereas the turbulence at the wing-tips is sustained. Hence, at $\mathrm{Re} \approx \mathrm{Re}_t$ the spot may split into two parts separated by a region of streaky structures.

Further flow visualization studies in plane Poiseuille flow were made by Alavyoon et al. [18]. They presented results that confirmed the results of Carlson et al. regarding the spot structure at low Reynolds numbers but showed that the splitting of the spot into two turbulent regions is a phenomenon occurring only at Reynolds numbers close to the transitional. The flow apparatus used by Alavyoon et al. also made it possible to obtain higher Re without obtaining natural transition. Results were presented that showed Reynolds number trends of spreading angle and propagation speeds (see Fig. 3a,b). The spreading angle was found to increase linearly with Re, from about 6° at $\mathrm{Re} = 1100$ to about 12° at $\mathrm{Re} = 2200$. The propagation speed of the rear interface shows a decreasing trend, whereas the front speed increases slightly for this Reynolds number range.

In the flow visualization studies mentioned above the spot shape is observed as a boundary between laminar and turbulent flow. The flow visualization method gives no information on the cross-channel variation. In the hot-wire measurements of Klingmann and Alfredsson [42], contour plots in the x–z-plane of the ensemble averaged streamwise velocity as well as the corresponding *rms* values were shown for various y-positions. The ensemble averaged mean velocity defines the spot shape and the *rms* gives the region of turbulent activity. The results shows that the cross-channel shape variation of the interface has an arrowhead shape with the largest extent on the channel centreline. Close to the wall both the width and the length are decreased. Turbulent activity is seen in the rear and central parts of the spot, indicating that the disturbances in the front part of the spot is passively convected downstream.

Velocity measurements of the flow field outside the wing-tip was carried out by Henningson and Alfredsson [43] with hot-film anemometry and it was shown that the waves observed in flow visualization appeared as regular wave-packets with a distinct frequency. It was shown that the streamwise velocity signal associated with the wave was antisymmetric with respect to the channel centreline ($y = 0$) which is in accordance with the behaviour of the least stable TS-waves in Poiseuille flow (see Fig. 4). Klingmann and Alfredsson [42] further investigated the waves and were able to show that they could be observed also within the turbulent wing-tip region where the streamwise velocity associated with the waves reached peak-to-peak amplitudes of $0.20U_{CL}$.

The hot-film measurements also showed that the mean flow around the spot is altered and that the flow tends to move around the spot, indicating that the spot acts as a flow blockage. Henningson and Alfredsson [43] analyzed the stability of the resulting flow field at $\mathrm{Re} = 1500$ for an oblique wave, using the Orr–Sommerfeld equation (see Eq. 3) with an effective velocity profile of the form

$$U + W \tan \phi$$

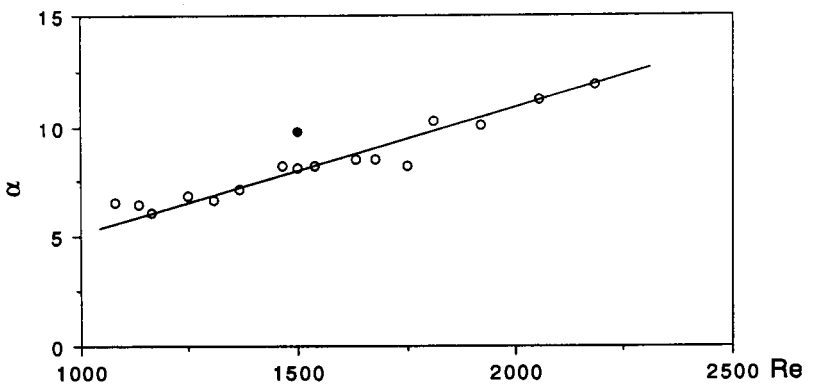

(a)

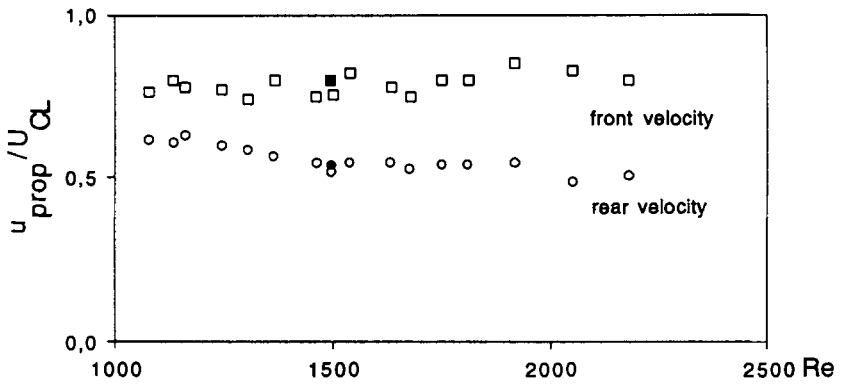

(b)

Fig. 3. Half-spreading angle (a) and propagation speeds of rear and front interfaces (b) as function of Reynolds number for spots in plane Poiseuille flow. Data from: Alavyoon et al. [18] open symbols and Henningson et al. [41] closed symbols.

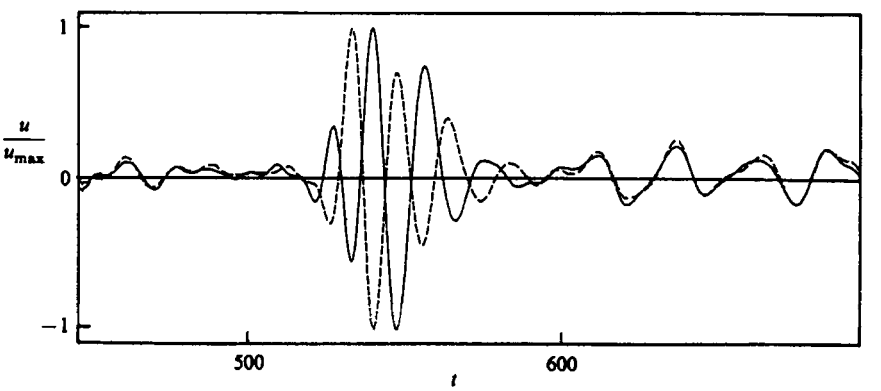

Fig. 4. High-pass filtered streamwise velocity signals measured simultaneously at $y = \pm 0.7$ in the wing tip region where waves were observed, showing the anti-symmetric property of the u-disturbance. From Henningson and Alfredsson [43].

where ϕ is the angle between the wave vector and the x-direction. This may give rise to 'cross-flow' inflectional profiles which could lead to rapid exponential growth. By using the measured velocity field and assuming a quasi-stationary velocity profile they showed that for the observed wave angles the mean flow outside the wing-tip of the spot was indeed unstable at $\mathrm{Re} = 1500$, however the growth rate was too small to explain the experimentally determined rapid growth of the waves.

A full numerical simulation at $\mathrm{Re} = 1500$ was reported by Henningson, Spalart and Kim [41] (see also Henningson and Kim [44]). The simulation showed in general good agreement with the experiments of Alavyoon et al. [18]. The propagation speed of the rear and front parts of the turbulent region agreed with experiments, whereas the spreading rate was somewhat too large. This may have been caused by interaction with neighbouring spots resulting from the periodic boundary conditions imposed in the simulation. The typical Poiseuille spot behaviour was observed where the front was relaminarized and the turbulence was maintained in the rearward part of the spot. Also the waves at the wingtips were reproduced in the simulation (see Fig. 5).

Henningson [45] analyzed the growth of the TS-waves outside the wing-tip further, now using the numerical data base of the spot simulation. The analysis was based on kinematic wave theory where waves are traced along group velocity rays. In this manner wave energy focusing resulting from the slowly varying mean flow outside the spot could also be taken into account. An inflectional 'cross-flow' instability was found to be the dominating growth mechanism and good agreement with the results for the wave growth extracted from the numerical simulation data was obtained.

A different approach to modelling the flow and wave field around the spot was taken by Li and Widnall [46] following the original idea of Widnall [47]. She assumed that the spot could be modelled by a region of Reynolds stress propagating with a certain speed, forcing the outside flow. Li and Widnall [46] argued that the non-linear forcing (RHS of Eq. 1a) was dominated by $\partial uv/\partial y$. They modelled this term with one symmetric and one anti-symmetric part with respect to the channel centreline. The symmetric term gave rise to a flow blockage effect, but no wave field was generated. This symmetry is what would be obtained for a fully developed turbulent mean flow. However, for anti-symmetric forcing a wave field was obtained that resembled the one seen in the experiments and the simulations.

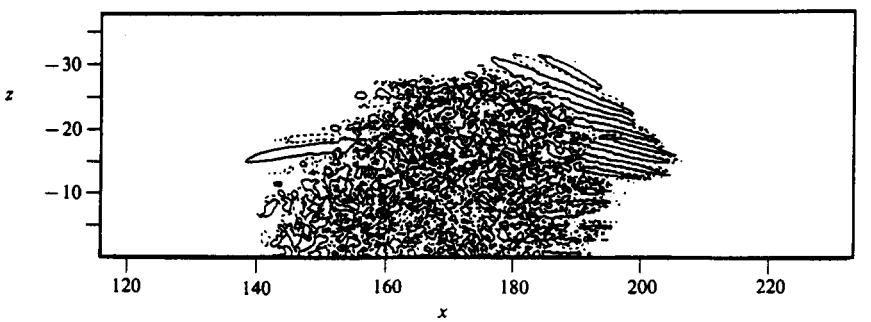

Fig. 5. The $\pm 0.01 U_{CL}$ contour lines of normal velocity in a horizontal plane at the channel centreline at $t = 258$. Dotted lines indicate negative values and solid lines positive. From Henningson and Kim [44].

3.3. Plane Couette flow

Studies of turbulent spots in plane Couette flow have only recently been carried out. Experimental studies of transition in plane Couette flow were however carried out earlier, but no consensus on even the transitional Re had been reached. The first reported study of turbulent spots was a direct numerical simulation carried out by Lundbladh and Johansson [7]. They created a turbulent spot by introducing a disturbance of high amplitude and followed its development in time. In this way they were also able to determine whether the Reynolds number was below or above the transitional value. At Re = 350 the disturbance decayed whereas at Re = 375 it was amplified and they concluded that the transitional Re was somewhere in between these two values. Simulations of spots were also carried out for Re = 750 and Re = 1500. In their study it was shown that the flow field around the turbulent spot was modified. Waves at the laminar turbulent interface near the widest part of the spot were also observed. However, in this case the wave crests are nearly aligned with the mean flow direction and only one or two wave-lengths could be observed outside the spot.

From the experimental point of view plane Couette flow is best studied in an apparatus with counter-moving walls. In such a set-up the net transport of fluid along the channel is zero and the fully developed state is reached on a diffusion determined timescale, h^2/ν. Tillmark and Alfredsson [8] constructed such an apparatus, with an infinite moving band acting as the walls. The moving band was transparent which made optical access to the channel possible for flow visualization. Using reflective flakes and a pointwise disturbance they measured spreading rates and propagation speeds of turbulent spots for Re up to 900. The transitional Reynolds number could be determined in several ways, as for instance running the channel at a high Re and decreasing the Re stepwise until turbulence could no longer be sustained in the channel. The transitional Re was in this case determined to 360. Also in the flow visualization, streamwise aligned waves were observed to travel out from the widest part of the spot. Figure 6 shows the spot shape in the xz-plane for both the experiment and the numerical simulation at Re = 750.

Close to the moving walls the spot extends further in the respective directions as compared to the centreline (Fig. 7). Thus, as seen from the lower wall we may say that there is an overhang in the streamwise direction close to the upper wall. This bears resemblance to the situation in the boundary layer case.

For low Reynolds numbers both the experiments and the simulations showed an increasing spreading rate with increasing Re. After the initial growth phase the spanwise spreading is larger than the streamwise and the spot tends towards a circular shape. For high Reynolds numbers (>700) an asymptotic spanwise spreading rate of just above 0.20 is reached. Figure 8 shows the spanwise width of the spot as function of time for various Re in the experiments of Tillmark and Alfredsson [8] together with simulation data of Lundbladh and Johansson [7]. Both from the simulation data as well as from the experiments it is clear that the spot shape is not self-similar.

From the simulation data it could be noted that the modification of the surrounding laminar flow is essentially two-dimensional in that it lacks a significant wall normal component. The magnitudes of the streamwise and spanwise deviations from the unperturbed values were, on the other hand, found to be substantial. This leaves room for speculation about growth by destabilization also for this flow situation, but has not yet been investigated in detail.

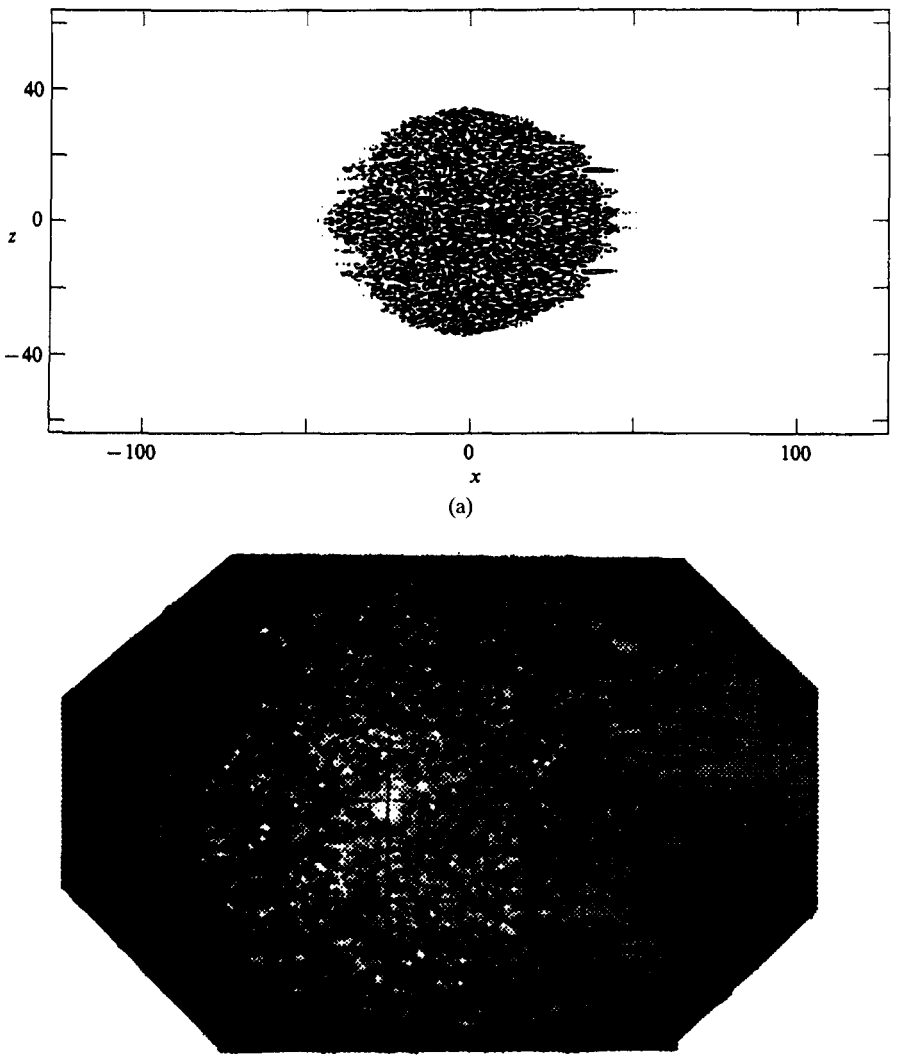

Fig. 6. Spot shape in plane Couette flow at Re = 750 at $t = 160$ after spot triggering. (a) Numerical simulation, showing v-contour lines at the plane $y = 0$ (from Lundbladh and Johansson [7]). (b) Flow visualization with reflecting flakes (from Tillmark and Alfredsson [8]).

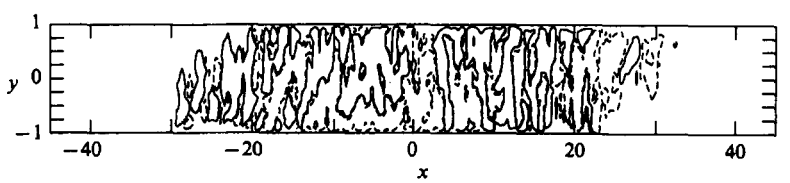

Fig. 7. Contours (± 0.02) of v in the mid x–y-plane at $t = 50$ and Re = 1500 (from Lundbladh and Johansson [7]).

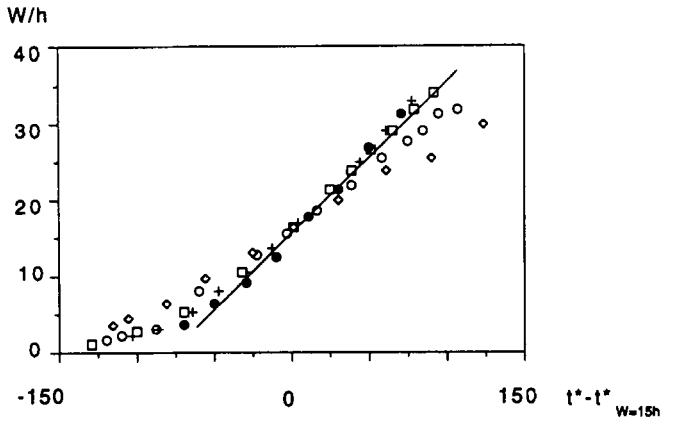

Fig. 8. Spot half-width, W, as a function of time. Time origin is set where $W/h = 15$. Data from experiments by Tillmark and Alfredsson [8], (◇): Re = 438, (○): Re = 521, (□): Re = 732, (+): Re = 943 and simulation by Lundbladh and Johansson [7], (●): Re = 750.

4. Turbulence characteristics in the interior of spots

The interior of turbulent spots exhibits a turbulence structure that is in many respects similar to that of the corresponding fully developed turbulent flow. This may be expected when the wall-parallel extent of the spot is many times larger than the wall-normal extent, and hence a large number of macroscales can be contained within the turbulent part of the spot. Wygnanski et al. [48] showed that the mean velocity profile in the boundary-layer spot exhibits the same kind of logarithmic behaviour as in the turbulent boundary layer, despite the fact that there is a slow spatial variation through the spot in quantities such as the wall friction. One should remember also that the Reynolds number normally is quite low in the interior of a spot. A friction velocity Reynolds number, $R_* = U_\tau \delta/\nu$ (or $U_\tau h/\nu$ in the channel flow cases), may be as low as 50.

In experimental investigations the turbulence statistics in the interior of spots are determined from ensemble averages of typically several hundred spot realizations. Intensities and higher moments are then determined from the fluctuations around the ensemble averages. In studies using direct numerical simulations this technique is of course not feasible. Flow characteristics can still be determined with a reasonable accuracy by spatial filtering or averaging techniques.

In the studies of Henningson and Kim [44] and Lundbladh and Johansson [7] of Poiseuille flow and Couette flow spots, respectively, a spatial filter with a Gaussian hat filter function was used. The mean was defined by

$$\langle u(x, y, z)\rangle = \frac{1}{\pi(ab)^{1/2}} \int_{-\infty}^{\infty} \int_{-\infty}^{\infty} u(x+\xi, y, z+\zeta) f(\xi, \zeta)\, \mathrm{d}\xi\, \mathrm{d}\zeta\,, \tag{10a}$$

$$f(\xi, \zeta) = \mathrm{e}^{-(\xi/a)^2-(\zeta/b)^2}\,, \tag{10b}$$

or correspondingly in Fourier space

$$\langle \hat{u}(\alpha, y, \beta)\rangle = \hat{f}(\alpha, \beta)\hat{u}(\alpha, y, \beta)\,. \tag{11}$$

In the Poiseuille flow case a and b were chosen as 3.5 and 2.5, respectively, and in the

Couette case they were both taken as $8/\pi \approx 2.55$. Various values of the filter length scale were tested, and the results were shown to be rather insensitive to the choice of this length scale. In the Couette case the filter function is larger than $1/e$ within a circle of diameter of approximately 5 half-heights. This is considerably smaller than the width of the analyzed spots, which was about 69 half-heights. Hence, also the global variations of the turbulence statistics within the spot can be determined with this technique.

Turbulence intensities are determined from the simulation data by applying the Gaussian filter to the squared disturbance field, defined as the deviation from the spatially averaged velocity field, e.g. $u_{rms} = \langle (u - \langle u \rangle)^2 \rangle^{1/2}$. Statistics averaged over the central part of the spot can then be obtained either by averaging this u_{rms} field or by applying a Gaussian filter with large values of a and b to the $u - \langle u \rangle$ field.

4.1. Turbulence statistics in the central part of the interior

Whereas the flow in the investigated Poiseuille and Couette flow spots corresponds to very low friction Reynolds numbers, considerably higher R_*-values have been reached in some studies of boundary-layer spots. In the investigation of Johansson et al. [49] detailed comparisons were made between the flow inside spots at $R_* \approx 1000$ and the fully turbulent boundary layer flow. A close adherence to standard turbulent boundary layer behaviour was shown for the statistics measured in the boundary layer spot. Also turbulence structure related information was investigated in the study of Johansson et al. and found to be practically identical to that of the turbulent boundary layer.

Poiseuille flow

The studies of Poiseuille flow spots (e.g. Carlson et al. [6], Alavyoon et al. [18], Klingmann and Alfredsson [42], Henningson and Kim [44]) have been carried out for Reynolds numbers (hU_{CL}/ν) in the range 1000–2200. Most of the efforts have been focused for Reynolds numbers of 1500–1600. One should note that Nishioka and Asai [50] found self-sustained turbulence only for Reynolds numbers above approximately 1600.

Klingmann and Alfredsson [42] constructed ensemble averages of the interior flow of Poiseuille spots from measurements with a hot-wire probe. They presented the results in space-like coordinates $(X, Z) = (x/tU_{CL},\ z/tU_{CL})$, which also enables comparison with the numerical simulation results of Henningson and Kim [44] where the Reynolds number was chosen as 1500. Figures (9a, b) show a comparison of isocontours of the streamwise mean velocity in the mid-plane ($y = 0$) as obtained from the physical and numerical experiments, respectively.

Despite the low R_* of about 70 in these cases the low-speed streak spacing in the viscous sublayer and other features of the turbulence structure in the central part of the spot is similar to that of a fully developed turbulent flow. It may be noteworthy that the R_* here is not much larger than that of the undisturbed laminar flow ($\approx$50). The mean velocity and streamwise turbulence intensity from the experiments of Klingmann and Alfredsson [42] are shown in Fig. 10. The general behaviour and quantitative data, such as the maximum turbulence streamwise intensity, are close to that found in fully developed turbulent channel flow. Henningson and Kim also showed detailed comparisons of shear-layer structures in the buffer region closely resembling results for fully turbulent channel flow.

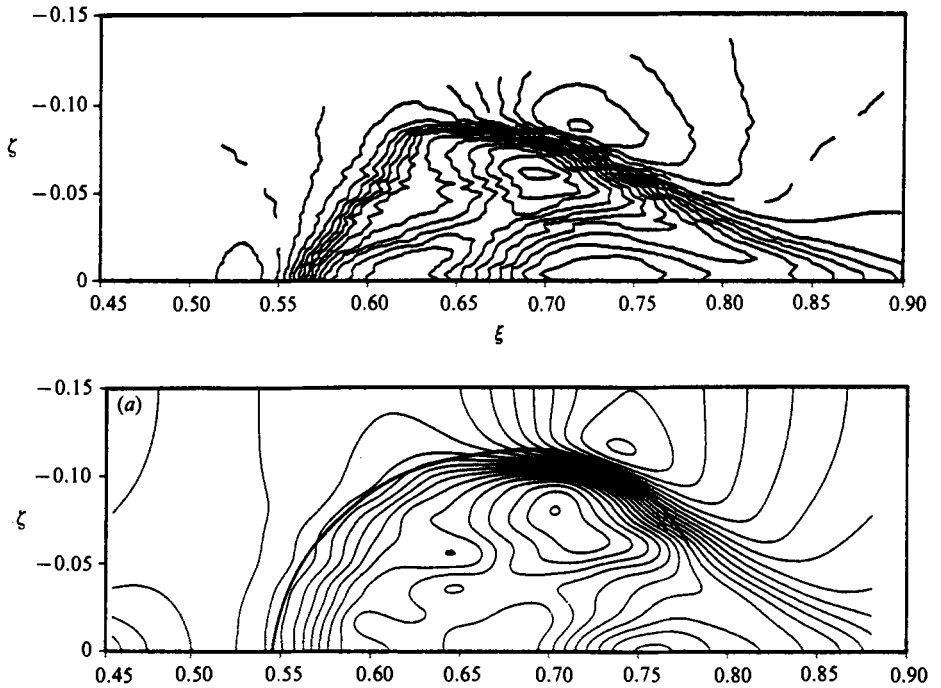

Fig. 9. Iso-contours of streamwise mean velocity from (a) the experiments of Klingmann and Alfredsson [42] at $x = 195$ and (b) the simulations of Henningson and Kim [44] at $t = 258$.

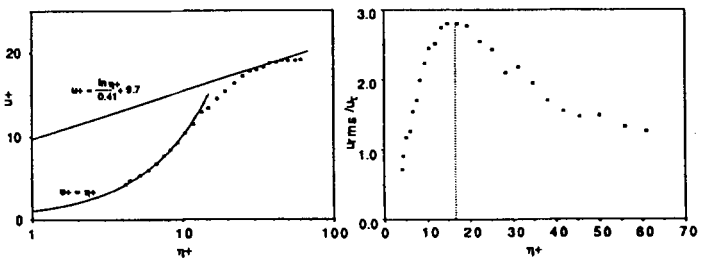

Fig. 10. Profiles of streamwise mean velocity and turbulence intensity from the central region of the Poiseuille spot ($x = 195$) (from Klingmann and Alfredsson [42]).

Couette flow

The spatially averaged velocity fields of Lundbladh and Johansson [7] for a Couette flow spot show an interesting pattern of the disturbance of the laminar region around the spot (Fig. 11). Essentially no normal velocity disturbance is present in the laminar region so the outer contour of $\langle v \rangle$ can also be taken as the outer edge of the spot. The higher wall friction inside the spot manifests itself in a weak flow towards the lower surface in the rear half of the interior, balanced by an upward flow in the forward part.

The spatially averaged mean velocity profile in the central region were also shown to exhibit the typical s-shape of turbulent Couette profiles. Profiles of the turbulence intensities for the central region were obtained by averaging over a large part of the central region of the spot (Fig. 12) simply through use of a large filter length. The maximum of u_{rms}/u_τ is about 2.4, and is found at $y^+ \approx 12$ which is quite low in comparison with the standard value

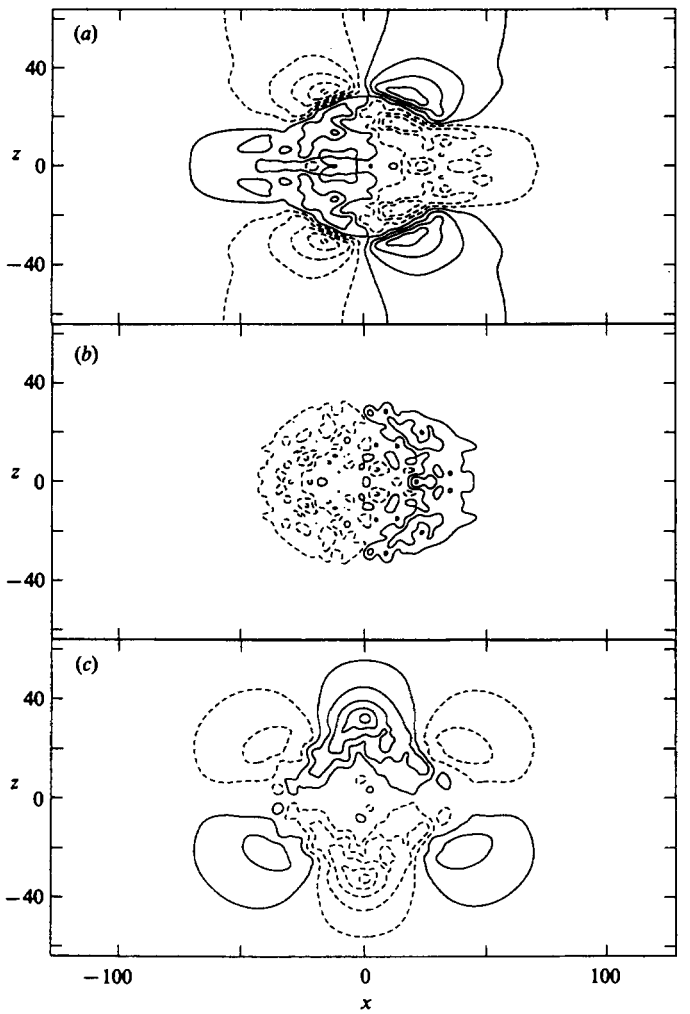

Fig. 11. Spatially averaged (a) u, (b) v and (c) w at the mid-plane ($y = 0$) at $t = 160$ (normalized by half-height (h) and U_w = half the total velocity difference between upper and lower surface ($\mathrm{Re} = hU_w/\nu = 750$) (from Lundbladh and Johansson [7]).

of about 2.8 from high Reynolds number experiments of channel and boundary layer flows. The v-intensity at this low Reynolds number has its maximum level at the centreline.

The fluctuation intensities of u on the centreline are only about 20% lower than the maximum near the wall. For lower Reynolds numbers it was shown to be even smaller. This is in contrast to e.g. high Reynolds number turbulent channel flow, where the centreline u-intensity is three times smaller than the maximum near the wall (Johansson and Alfredsson [51]). One should note that R_* is as low as 54 in this Couette flow case. The low Reynolds number is one reason for the high value of u_{rms} at the centreline and the relatively small difference between the centre and near wall maximum levels. A further reason is the fact that for Couette flow, in contrast to e.g. channel flow, the mean velocity gradient is non-zero at the centreline, giving a non-zero turbulence production there. This gives an especially significant effect at this low Reynolds number.

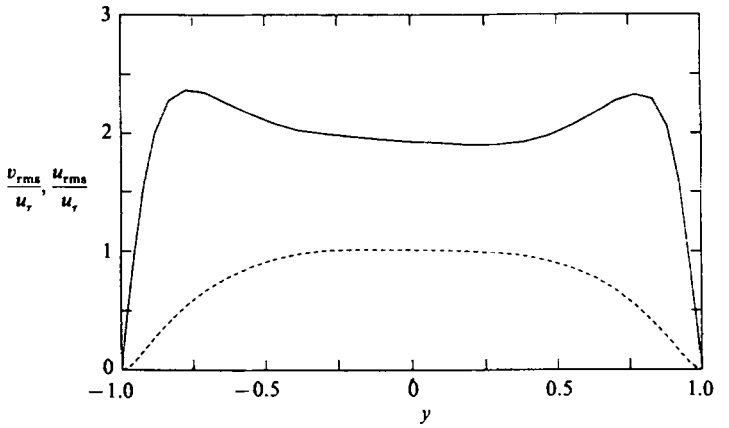

Fig. 12. Turbulence intensity profiles averaged over a large part of the central region of the Couette spot at $t = 160$ (Re = 750) (from Lundbladh and Johansson [7]).

4.2. Regions of enhanced turbulence intensities

For the Couette spot the edge region close to the laminar-turbulent interface exhibits a considerably higher turbulence intensity than the central part (Lundbladh and Johansson [7]).

The Poiseuille flow spot has a wing-tip region of enhanced activity as shown both in the experiments (Klingmann and Alfredsson [42]) and the simulations (Henningson and Kim [44]). Figure 13a shows the ensemble averaged intensity in a horizontal plane. The areas used to construct central part averages and wing-tip averages are enclosed by thick lines. Intensity profiles averaged over the central part and wing-tip region, respectively, are shown in Fig. 13. One may note that, in particular, the v and w components show significantly higher levels in the wing-tip region. This is coupled to the wave-activity in this region, as discussed earlier. Henningson and Kim also showed that there is a significantly larger activity in this region in terms of appearance of shear-layer structures in the buffer region. These have earlier been shown to be strongly coupled to high levels of turbulence production (see e.g. Johansson et al. [52]).

5. Final remarks

A number of investigations into the formation and development of turbulent spots in channel flows have been reviewed. There are three main observations that one can draw from this review. Firstly, the initial development is associated with the transient growth due to the three-dimensional lift-up effect. Secondly, the spreading and propagation velocities of the different spots are quite similar. Thirdly, the velocity field inside the spots show essentially all the characteristics of fully developed turbulent flow, albeit at low Reynolds numbers.

The mechanism behind the rapid spreading of the spots is not yet fully understood. However, observations of wave activity, modifications of the surrounding flow field and stability calculations point in the direction of a growth by destabilization mechanism in all of the flow situations reviewed here.

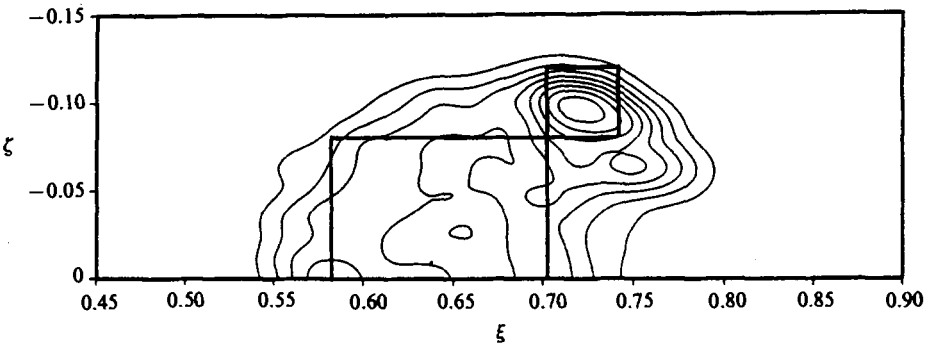

(a)

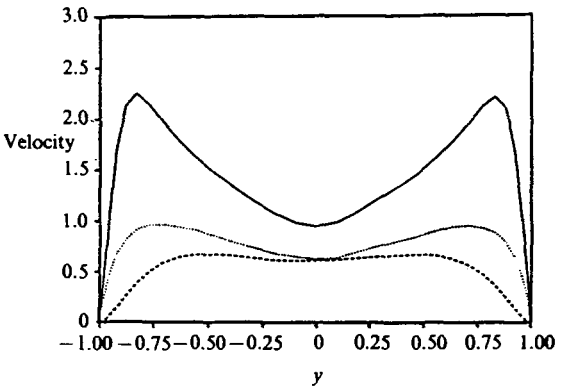

(b)

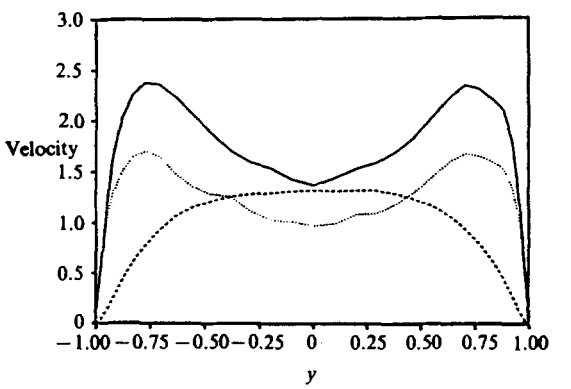

(c)

Fig. 13. Turbulence intensities for the Poiseuille spot. (a) Spatially averaged streamwise intensity in the $y = 0.83$ plane. (b) Profiles of u_{rms}/u_τ (solid curve), v_{rms}/u_τ (dashed curve) and w_{rms}/u_τ (dotted curve), averaged over the central region (large rectangle) (c) Profiles of u_{rms}/u_τ, v_{rms}/u_τ and w_{rms}/u_τ, averaged over the wing-tip region (small rectangle) ($t = 258$, Re = 1500) (from Henningson and Kim [44]).

Acknowledgement

We wish to thank Barbro Klingmann, Anders Lundbladh and Nils Tillmark for the contributions they have made to the research reviewed here. We also wish to express gratitude for the support from the Swedish National Board for Industrial and Technical Development (NUTEK) and the Swedish Research Council for the Engineering Sciences (TFR).

Notes

[1] Also at The Aeronautical Research Institute of Sweden (FFA), Box 11021, S-16111 Bromma, Sweden.
[2] The Reynolds–Orr equation is not valid for water table flow because of the free surface boundary condition. This is also why an amplitude independent Re_g cannot be found for that case.

References

1. P.S. Klebanoff, K.D. Tidstrom and L.M. Sargent, The three-dimensional nature of boundary layer instability. *J. Fluid Mech.* 12 (1962) 1–34.
2. T. Herbert, Secondary instability of boundary layers. *Ann. Rev. Fluid Mech.* 20 (1988) 487–526.
3. M.V. Morkovin, The many faces of transition. In C.S. Wells, editor, *Viscous Drag Reduction*. Plenum Press (1969).
4. H.W. Emmons, The laminar-turbulent transition in a boundary layer – Part I. *J. Aero. Sci.* 18 (1951) 490–498.
5. J.J. Riley and M. Gad-el Hak, The dynamics of turbulent spots. In *Frontiers of Fluid Mechanics*, pages 123–155. Springer (1985).
6. D.R. Carlson, S.E. Widnall and M.F. Peeters, A flow visualization study of transition in plane Poiseuille flow. *J. Fluid Mech.* 121 (1982) 487–505.
7. A. Lundbladh and A.V. Johansson, Direct simulation of turbulent spots in plane Couette flow. *J. Fluid Mech.* 229 (1991) 499–516.
8. N. Tillmark and P.H. Alfredsson, Experiments on transition in plane Couette flow. *J. Fluid Mech.* 235 (1992) 89–102.
9. J. Amini and G. Lespinard, Experimental study of an "incipient spot" in a transitional boundary layer. *Phys. Fluids* 25 (10) (1982) 1743–1750.
10. M. Gaster and I. Grant, An experimental investigation of the formation and development of a wave packet in a laminar boundary layer. *Proc. Roy. Soc. Lond. Ser. A* 347 (1975) 253–269.
11. F.W. Chambers and A.S.W. Thomas, Turbulent spots, wave packets and growth. *Phys. Fluids* 26 (1983) 1160–1162.
12. M.S. Acarlar and C.R. Smith, A study of hairpin vortices in a laminar boundary layer. Part 2. Hairpin vortices generated by fluid injection. *J. Fluid Mech.* 175 (1987) 43–48.
13. N.D. Sandham and L. Kleiser, The late stages of transition to turbulence in channel flow. *J. Fluid Mech.* 245 (1992) 319–348.
14. K.S. Breuer and J.H. Haritonidis, The evolution of a localized disturbance in a laminar boundary layer. Part I: Weak disturbances. *J. Fluid Mech.* 220 (1990) 569–594.
15. J. Cohen, K.S. Breuer and J.H. Haritonidis, On the evolution of a wave packet in a laminar boundary layer. *J. Fluid Mech.* 225 (1991) 575–606.
16. D.D. Joseph and S. Carmi, Stability of Poiseuille flow in pipes, annuli and channels. *Quart. Appl. Math.* 26 (1969) 575–599.
17. D.D. Joseph, Nonlinear stability of the Boussinesq equations by the energy method. *Arch. Rat. Mech. Anal.* 22 (1966) 163–184.
18. F. Alavyoon, D.S. Henningson and P.H. Alfredsson, Turbulent spots in plane Poiseuille flow – flow visualization. *Phys. Fluids* 29 (1986) 1328–1331.
19. L.H. Gustavsson and J.-E. Ögren, Observations of turbulent spots on a water table. TECHNICAL REPORT 1982:039 T, Department of Mechanical Engineering, Luleå University of Technology, Sweden (1982).
20. S.A. Orszag, Accurate solution of the Orr–Sommerfeld stability equation. *J. Fluid Mech.* 50 (1971) 689–703.
21. I.H. Herron, Observations on the role of vorticity in the stability of wall bounded flows. *Stud. Appl. Math.* 85 (1991) 269–286.

22. R.W.-Y. Chin, *Stability of flows down an inclined plane*. PhD thesis, Harvard University, Division of Applied Sciences, Cambridge, Mass (1981).
23. L.H. Gustavsson, Excitation of direct resonances in plane Poiseuille flow. *Stud. Appl. Math.* 75 (1986) 227–248.
24. S.C. Reddy and D.S. Henningson, Energy growth in viscous channel flows. *J. Fluid Mech.* 252 (1993) 209–238.
25. K.M. Butler and B.F. Farrell, Three-dimensional optimal perturbations in viscous shear flow. *Phys. Fluids A* 4 (1992) 1637–1650.
26. M. Gaster, The development of three-dimensional wave packets in a boundary layer. *J. Fluid Mech.* 32 (1968) 173–184.
27. M. Gaster, A theoretical model for the development of a wave packet in a laminar boundary layer. *Proc. Roy. Soc. Lond. Ser. A* 347 (1975) 271–289.
28. L.H. Gustavsson, Energy growth of three-dimensional disturbances in plane Poiseuille flow. *J. Fluid Mech.* 224 (1991) 241–260.
29. D.S. Henningson, A. Lundbladh and A.V. Johansson, A mechanism for bypass transition from localized disturbances in wall bounded shear flows. *J. Fluid Mech.* 250 (1993) 169–207.
30. T. Ellingsen and E. Palm, Stability of linear flow. *Phys. Fluids* 18 (1975) 487–488.
31. M.T. Landahl, A note on an algebraic instability of inviscid parallel shear flows. *J. Fluid Mech.* 98 (1980) 243–251.
32. D.S. Henningson, The inviscid initial value problem for a piecewise linear mean flow. *Stud. Appl. Math.* 78 (1988) 31–56.
33. M.T. Landahl, Wave breakdown and turbulence. *SIAM J. Appl. Math*, 28 (1975) 735–756.
34. L.H. Gustavsson, *On the evolution of disturbances in boundary layer flows*. PhD thesis, Royal Institute of Technology, Stockholm, Sweden (1978) (TRITA-MEK 78-02).
35. D.S. Henningson, A.V. Johansson and A. Lundbladh, On the evolution of localized disturbances in laminar shear flows. In D. Arnal and R. Michel, editors, *Laminar-Turbulent Transition*, pp. 279–284 (1990) Springer Verlag.
36. B.G.B. Klingmann, On transition due to three-dimensional disturbances in plane Poiseuille flow. *J. Fluid Mech.* 240 (1992) 167–195.
37. M. Gad-el-Hak, R.F. Blackwelder and J.J. Riley, On the growth of turbulent regions in laminar boundary layers. *J. Fluid Mech.* 110 (1981) 73–95.
38. M. Mitchner, Propagation of turbulence from an instantaneous point disturbance. *J. Aero. Sci.* 21 (1954) 350–351.
39. J.R. Bertshy and F.H. Abernathy, Modifications to laminar and turbulent boundary layers due to the addition of dilute polymer solutions. In *Drag Reduction*, Second International Conference on Drag Reduction, Cambridge, UK (1977) BHRA Fluid Engineering.
40. P.Å. Lindberg, E.M. Fahlgren, P.H. Alfredsson and A.V. Johansson, An experimental study of the structure and spreading of turbulent spots. In V. Kozlov, editor, *Laminar-Turbulent Transition*, pp. 617–624 (1985) Springer-Verlag.
41. D.S. Henningson, P. Spalart and J. Kim, Numerical simulations of turbulent spots in plane Poiseuille and boundary layer flows. *Phys. Fluids* 30 (1987) 2914–2917.
42. B.G.B. Klingmann and P.H. Alfredsson, Turbulent spots in plane Poiseuille flow – measurements of the velocity field. *Phys. Fluids A* 2 (1990) 2183–2195.
43. D.S. Henningson and P.H. Alfredsson, The wave structure of turbulent spots in plane Poiseuille flow. *J. Fluid Mech.* 178 (1987) 405.
44. D.S. Henningson and J. Kim, On turbulent spots in plane Poiseuille flow. *J. Fluid Mech.* 228 (1991) 183–205.
45. D.S. Henningson, Wave growth and spreading of a turbulent spot in plane Poiseuille flow. *Phys. Fluids A* 1 (1989) 1876–1882.
46. F. Li and S.E. Widnall, Wave patterns in plane Poiseuille flow created by concentrated disturbances. *J. Fluid Mech.* 208 (1989) 639–656.
47. S.E. Widnall, Growth of turbulent spots in plane Poiseuille flow. In T. Tatsumi, editor, *Turbulence and chaotic phenomena in fluids*, pp. 93–98 (1984) Elsevier.
48. I. Wygnanski, M. Sokolov and D. Friedman, On transition in a pipe. Part 2. The equilibrium puff. *J. Fluid Mech.* 69 (1975) 283–304.
49. A.V. Johansson, J. Her and J.H. Haritonidis, On the generation of high amplitude wall-pressure peaks in turbulent boundary layers and spots. *J. Fluid Mech.* 175 (1987) 119–142.
50. M. Nishioka and M. Asai, Some observations of the subcritical transition in plane Poiseuille flow. *J. Fluid Mech.* 150 (1985) 441–450.
51. A.V. Johansson and P.H. Alfredsson, On the structure of turbulent channel flow. *J. Fluid Mech.* 122 (1982) 295–314.
52. A.V. Johansson, P.H. Alfredsson and J. Kim, Evolution and dynamics of shear-layer structures in near-wall turbulence. *J. Fluid Mech.* 224 (1991) 579–599.